

MicroRNA-873 targets HOXA9 to inhibit the aggressive phenotype of osteosarcoma by deactivating the Wnt/ β -catenin pathway

YILIN LIU, YUQIANG WANG, HAO YANG, LIANG ZHAO,
RUIPENG SONG, HONGYU TAN and LIMIN WANG

Department of Orthopedics, The First Affiliated Hospital of Zhengzhou University,
Zhengzhou, Henan 450052, P.R. China

Received November 1, 2018; Accepted January 25, 2019

DOI: 10.3892/ijo.2019.4735

Abstract. Several microRNAs (miRNAs or miRs) that regulate a variety of cancer-related events are dysregulated in osteosarcoma (OS). An exploration of the specific roles of miRNAs in OS is crucial for the identification of suitable therapeutic targets. Previous studies have shown that miR-873 plays tumor suppressive or oncogenic roles in different types of cancer. However, whether miR-873 is implicated in OS carcinogenesis and cancer progression remains poorly understood. In the present study, we demonstrated that the miR-873 levels were decreased in OS tissues and cell lines. The decreased expression of miR-873 was related to tumor size, clinical stage and distant metastasis in patients with OS. The introduction of miR-873 significantly inhibited tumor cell proliferation, migration and invasion *in vitro*, promoted apoptosis *in vitro* and restricted tumor growth *in vivo*. Furthermore, homeobox A9 (*HOXA9*) was validated as a direct target gene of miR-873 in OS cells. *HOXA9* was markedly expressed in OS tissues, and its upregulation inversely correlated with the miR-873 levels. Moreover, *HOXA9* silencing produced similar effects as observed with miR-873 overexpression in OS cells. Consistently, the exogenous expression of *HOXA9* partially reversed the suppression of the aggressive phenotype induced by miR-873 overexpression in OS cells. Notably, miR-873 was able to deactivate the Wnt/ β -catenin pathway in OS cells by regulating *HOXA9*, both *in vitro* and *in vivo*. On the whole, the present study demonstrates that miR-873 suppresses the development of OS by directly targeting *HOXA9* and inhibiting the Wnt/ β -catenin pathway, and suggests that

miR-873 may prove to be useful as a diagnostic biomarker of OS, as well as in the development of novel therapies.

Introduction

Osteosarcoma (OS), an aggressive and malignant neoplasm originating from primitive transformed mesenchymal cells, affects 4-5 individuals per million (1-3). It can occur in any human bone, although it is predominant in the distal femur, the proximal tibia, and the proximal humerus (4). OS is characterized by a high malignancy, high destructivity, frequent relapses and a strong propensity to metastasize into lung cancer (5). Considerable advances have been made in the therapeutic strategies for the treatment of OS, including neoadjuvant or adjuvant chemotherapy combined with surgery and radiotherapy. However, the prognosis of patients with OS remains unsatisfactory, with a 5-year survival rate of 30% (6,7). The formation and progression of OS is a complex process involving a variety of molecular alterations related to critical signal transduction pathways. However, the precise molecular mechanisms underlying OS pathogenesis remain unclear (8,9). Therefore, the elucidation of these mechanisms is an urgent requirement for the development of novel treatment strategies for patients suffering from this aggressive malignancy.

MicroRNAs (miRNAs or miRs) are a subset of endogenous, non-coding, short RNA molecules of 22-28 nucleotides in length (10). They serve as key regulators of gene expression by complete or partial binding to the 3'-untranslated regions (3'-UTRs) of target genes, causing mRNA degradation or translation inhibition (11). A single miRNA is able to modulate numerous target genes, and it is estimated that approximately 30% of human protein-coding genes are modulated by miRNAs (12,13). A wide range of biological processes, such as cell proliferation, apoptosis, the cell cycle, metastasis and angiogenesis, are regulated by miRNAs (14). Changes in miRNA expression profiles have been identified in almost all types of human cancer including OS (15), gastric cancer (16), breast cancer (17) and glioma (18). Numerous miRNAs have recently been reported to be dysregulated in OS, and differentially expressed miRNAs may contribute to OS carcinogenesis and progression by acting as oncogenes

Correspondence to: Professor Yilin Liu, Department of Orthopedics, The First Affiliated Hospital of Zhengzhou University, 1 Jianshe East Road, Zhengzhou, Henan 450052, P.R. China
E-mail: yilinliu_orth@126.com

Key words: osteosarcoma, microRNA-873, homeobox A9, Wnt/ β -catenin pathway

or tumor suppressors (19,20). Therefore, miRNA-based therapeutic techniques represent promising modalities for the treatment of patients with OS.

Previous studies have demonstrated that miR-873 is one of the miRNAs involved in cancer, and plays a tumor suppressive or oncogenic role in various types of human cancer (21-28). However, whether miR-873 is implicated in OS carcinogenesis and cancer progression remains poorly understood. Thus, the aim of the present study was to assess miR-873 expression in OS and to examine the effects of miR-873 overexpression on cellular processes. We also explored the molecular mechanisms involved in the miR-873-induced regulation of malignant progression in OS.

Materials and methods

Patients and tissue specimens. A total of 49 paired OS tissues and adjacent normal bone tissues were obtained from the First Affiliated Hospital of Zhengzhou University (Zhengzhou, China) between July, 2015 and August, 2017. All patients received surgical resection and had not been treated with chemotherapy, radiotherapy, or any other therapy prior to surgery. Freshly resected tissue samples were immediately frozen in liquid nitrogen and stored at -80°C until use. The Ethics Committee of the First Affiliated Hospital of Zhengzhou University approved this study, and all patients provided written informed consent.

Cells and cell culture. We purchased a normal human osteoblast (hFOB1.19) and 4 human OS cell lines (MG-63, SAOS-2, HOS and U2OS) from the American Type Culture Collection (ATCC, Manassas, VA, USA). All the cell lines were cultured in Dulbecco's modified Eagle's medium (DMEM) supplemented with 10% fetal bovine serum (FBS) and a 1% mixture of penicillin/streptomycin (all from Gibco/Invitrogen/Thermo Fisher Scientific, Waltham, MA, USA). The cells were maintained at 37°C in a humidified atmosphere containing 5% CO_2 .

Oligonucleotide and plasmid transfection. We obtained miR-873 mimics and negative control miRNA mimics (miR-NC) from RiboBio (Guangzhou, China). Small interfering RNA for *HOXA9* (*HOXA9* siRNA) and negative control siRNA (NC siRNA) were chemically synthesized by Shanghai GenePharma Co., Ltd. (Shanghai, China). The *HOXA9* overexpression plasmid, pcDNA3.1-*HOXA9* (pc-*HOXA9*), and an empty pcDNA3.1 plasmid were generated by Integrated Biotech Solutions (Shanghai, China). The cells were plated in 6-well plates at a density of 6×10^5 cells/well. When the cells reached 70-80% confluence, the above-mentioned mimics, siRNA, or plasmids were used for cell transfection with Lipofectamine 2000 (Invitrogen/Thermo Fisher Scientific), according to the manufacturer's instructions. Reverse transcription-quantitative polymerase chain reaction (RT-qPCR) and cell counting kit-8 (CCK-8) assay, colony formation assay and tumor xenograft assay were performed on transfected cells following 24 h of incubation at 37°C with 5% CO_2 . At 48 h post-transfection, flow cytometric analysis and Transwell migration and invasion assays were carried out. Following 72 h of culture, western blot analysis was used for the determination of protein expression.

RT-qPCR. Total RNA was isolated from the tissue samples and cells using TRIzol reagent (Invitrogen/Thermo Fisher Scientific). Total RNA was used to determine miR-873 expression by reverse transcription using a TaqMan MicroRNA Reverse Transcription kit (Applied Biosystems, Foster City, CA, USA). The temperature protocol for reverse transcription was as follows: 16°C for 30 min, 42°C for 30 min and 85°C for 5 min. Thereafter, we carried out quantitative PCR (qPCR) using a TaqMan MicroRNA PCR kit (Applied Biosystems). The temperature protocol for qPCR was as follows: 50°C for 2 min, 95°C for 10 min; 40 cycles of denaturation at 95°C for 15 sec; and annealing/extension at 60°C for 60 sec. To determine *HOXA9* mRNA expression, we prepared complementary DNA from total RNA using a PrimeScript RT reagent kit (Takara Bio, Dalian, China). The thermocycling conditions for reverse transcription were as follows: 37°C for 15 min and 85°C for 5 sec. Subsequently, qPCR was performed using a SYBR Premix Ex Taq™ kit (Takara Bio). The thermocycling conditions for qPCR were as follows: 5 min at 95°C , followed by 40 cycles of 95°C for 30 sec and 65°C for 45 sec. The relative expression levels of miR-873 and *HOXA9* mRNA were normalized to the endogenous controls, U6 small nuclear RNA and GAPDH, respectively. The primers were designed as follows: miR-873, 5'-CTGCACTCCCCACCTG-3' (forward) and 5'-GTGCAGGGTCCGAGGT-3' (reverse); U6, 5'-GCTTC GGCAGCACATATACTAAAAT-3' (forward) and 5'-CGCTT CACGAATTTGCGTGTTCAT-3' (reverse); *HOXA9*, 5'-CAA CAAAGACCGAGCAAA-3' (forward) and 5'-ATACCTCCT CCATCAAAGC-3' (reverse); and GAPDH, 5'-TCCCATCAC CATCTTCCA-3' (forward) and 5'-CATCAGCCACAGTT TCC-3' (reverse). Gene expression was analyzed using the $2^{-\Delta\Delta\text{C}_q}$ method (29).

CCK-8 assay. The transfected cells were incubated at 37°C in 5% CO_2 for 24 h, harvested, and seeded into 96-well plates at a density of 3×10^3 cells/well. Cellular proliferation was determined at the following time points following inoculation: 0, 24, 48 and 72 h. Specifically, the cells were treated with 10 μl of CCK-8 solution (Dojindo Molecular Technologies, Inc., Kumamoto, Japan), then incubated them at 37°C in 5% CO_2 for a further 2 h. The absorbance was detected at 450 nm using an Enzyme Immunoassay Analyzer (Bio-Rad Laboratories, Hercules, CA, USA).

Colony formation assay. At 24 h following transfection, the cells were collected and digested using 0.25% trypsin (Gibco/Invitrogen/Thermo Fisher Scientific) to produce a suspension of single cells. A total of 1×10^3 cells were seeded into 6-well plates, and incubated at 37°C in 5% CO_2 for 10 days. On day 11, the resulting colonies were washed with phosphate-buffered saline (PBS; Gibco/Invitrogen/Thermo Fisher Scientific), and fixed with 4% paraformaldehyde, and stained with methyl violet (Beyotime Institute of Biotechnology, Shanghai, China). Finally, the colonies were counted using an Olympus IX83 inverted microscope (Olympus Corp., Tokyo, Japan); a colony was defined as a group of >50 cells.

Flow cytometry analysis of the cell apoptosis rate. The proportion of apoptotic cells was evaluated using an Annexin V-fluorescein isothiocyanate (FITC) apoptosis

detection kit (Biolegend, San Diego, CA, USA). Briefly, the transfected cells were cultured in 6-well plates for 48 h, collected, and washed 3 times with cold PBS. The cells were then resuspended in 100 μ l of binding buffer, and double-labeled with 5 μ l Annexin V-FITC and 5 μ l propidium iodide. Following incubation at 37°C in the dark for 30 min, a flow cytometer (FACScan™; BD Biosciences, Franklin Lakes, NJ, USA) was used to determine the rate of cell apoptosis.

Transwell migration and invasion assays. For these assays, 8- μ m Transwell chambers (BD Biosciences) were used to determine the cell migratory ability. At 48 h following transfection, the cells were washed twice in PBS and suspended in FBS-free DMEM. A total of 5x10⁴ cells were seeded into the upper compartments, and the lower compartments were covered with 500 μ l of DMEM containing 10% FBS. Following cultivation for 48 h, the non-migrating or non-invading cells were wiped out using a cotton swab. The cells adhering to the lower surface of the Transwell insert were fixed with 4% paraformaldehyde, stained with 0.05% crystal violet (Beyotime Institute of Biotechnology), washed thrice with PBS, and air-dried. A Transwell invasion assay that was similar to the migration assay was carried out, except that the chambers were pre-coated with Matrigel (BD Biosciences) before the experiment began. Finally, the cells that had migrated or invaded were photographed, and we counted at least 5 representative fields/inserts under an inverted microscope (x200 magnification; IX83; Olympus Corp.).

Tumor xenograft assay. We obtained 4-5-week-old female nude mice (weighing 18-19 g) from the Shanghai Laboratory Animal Center (Chinese Academy of Sciences, Shanghai, China). All nude mice were housed in sterile and pathogen-free conditions (25°C; 50% humidity; 10-h light/14-h dark cycle). The HOS cells were transfected with miR-873 mimics or the miR-NC. At 24 h following transfection, we collected the cells and subcutaneously injected them into the upper flanks of each nude mouse (n=4 for each group). We calculated the volume of each tumor xenograft using the following formula: 1/2 x tumor length x tumor width². We sacrificed all the nude mice 30 days after seeding the HOS cells (at the time of sacrifice, the mice weighed approximately 27 g), and excised and measured the tumors. All experimental procedures were approved by the Ethics Review Committee of the First Affiliated Hospital of Zhengzhou University.

Bioinformatics analysis. We used the following three miRNA target prediction software packages to search for potential targets of miR-873: TargetScan 7.1 (<http://www.targetscan.org/>), miRanda (<http://www.microrna.org>) and miRDB (<http://www.mirdb.org/>).

Luciferase reporter assay. Human wild-type (wt) *HOXA9* 3'-UTR containing the predicted miR-873 binding site and the mutant (mut) *HOXA9* 3'-UTR were amplified by Shanghai GenePharma Co., Ltd., and sub-cloned into the pMIR-REPORT vector (Promega, Madison, WI, USA). We named the generated luciferase reporter plasmids pMIR-wt-*HOXA9*-3'-UTR and pMIR-mut-*HOXA9*-3'-UTR. We seeded the cells into 24-well plates (1.5x10⁵ cells/well) one night prior to transfection.

We introduced a mixture of pMIR-wt-*HOXA9*-3'-UTR, pMIR-mut-*HOXA9*-3'-UTR, and miR-873 mimics or miR-NC into the cells using Lipofectamine 2000 (Invitrogen/Thermo Fisher Scientific) in accordance with the manufacturer's instructions. The transfected cells were lysed and assayed for the detection of luciferase activity at 48 h post-transfection using a dual-luciferase reporter assay system (Promega). The activity of Firefly luciferase was normalized to that of *Renilla* luciferase.

Protein extraction and western blot analysis. The homogenized tissues were solubilized and the cells were cultured with radioimmunoprecipitation assay lysis buffer (Beyotime Institute of Biotechnology) to isolate the total protein. The protein concentration was quantified using a BCA kit (Beyotime Institute of Biotechnology). Subsequently, equal amounts of protein were loaded onto 10% polyacrylamide gels for sodium dodecyl sulfate-polyacrylamide gel electrophoresis (SDS-PAGE), transferred them to PVDF membranes (EMD Millipore, Billerica, MA, USA), and blocked the proteins at room temperature for 2 h with 5% skimmed milk diluted in Tris-buffered saline (TBS) containing 0.1% Tween-20 (TBST). Following overnight incubation at 4°C with primary antibodies, the membranes were washed thrice with TBST and probed with horseradish peroxidase-conjugated immunoglobulin G secondary antibodies (ab205719 and ab6721; 1:5,000 dilution; Abcam, Cambridge, UK) for 2 h at room temperature. Western blot analysis was carried out using a Pierce ECL Western Blotting substrate (Invitrogen/Thermo Fisher Scientific), according to the manufacturer's instructions. The following primary antibodies were used: Rabbit anti-human monoclonal *HOXA9* antibody (ab140631; 1:1,000 dilution; Abcam), mouse anti-human monoclonal β -catenin antibody (sc-59737; 1:1,000 dilution; Santa Cruz Biotechnology, Santa Cruz, CA, USA), mouse anti-human monoclonal p- β -catenin antibody (sc-57534; 1:1,000 dilution; Santa Cruz Biotechnology), rabbit anti-human monoclonal cyclin D1 antibody (ab134175; 1:1,000 dilution; Abcam) and rabbit anti-human GAPDH antibody (ab128915; 1:1,000 dilution; Abcam). The expression levels of the target proteins were normalized to those of GAPDH.

Statistical analysis. All data are expressed as the means \pm standard error from at least 3 independent experiments. Differences between pairs of groups were analyzed using the Student's t-test. One-way analysis of variance was used, followed by the Student-Newman-Keuls post hoc test to evaluate the differences between multiple groups. The correlation between the miR-873 and *HOXA9* mRNA levels in the OS tissues was determined by Spearman's correlation analysis. The Chi-square test was used to assess the association between miR-873 and the clinicopathological characteristics of the patients with OS. Statistical significance was set at P<0.05.

Results

miR-873 is downregulated in OS tissues and cell lines. To investigate the clinical value of miR-873 in OS, we first detected miR-873 expression in 49 pairs of OS tissues and adjacent normal bone tissues using RT-qPCR analysis. The results revealed the decreased expression of miR-873 in the

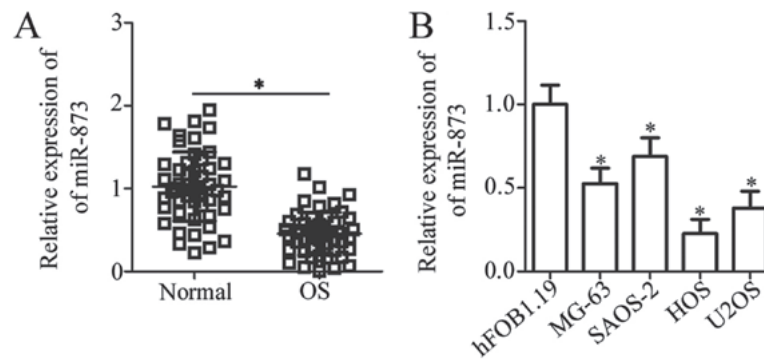


Figure 1. Expression of miR-873 in osteosarcoma (OS) tissues and cell lines. (A) We used reverse transcription-quantitative polymerase chain reaction (RT-qPCR) analysis to detect miR-873 expression in 49 pairs of OS tissues and adjacent normal bone tissues. * $P<0.05$ vs. adjacent normal bone tissues. (B) We used RT-qPCR to determine the expression levels of miR-873 in 4 OS cell lines (MG-63, SAOS-2, HOS and U2OS) and a normal human osteoblast (hFOB1.19). * $P<0.05$ vs. hFOB1.19 cells.

Table I. Association of miR-873 expression with the clinicopathological characteristics of the patients with OS.

Characteristics	miR-873 expression		P-value
	Low	High	
Age at diagnosis (years)			0.484
<18	16	13	
≥ 18	9	11	
Sex			0.482
Male	15	12	
Female	10	12	
Tumor size (cm)			0.015 ^a
<5	9	17	
≥ 5	16	7	
Clinical stage			0.032 ^a
I-IIA	8	15	
IIB/III	17	9	
Distant metastasis			0.015 ^a
Negative	7	15	
Positive	18	9	
Anatomic location			0.162
Tibia/femur	14	18	
Elsewhere	11	6	

^a $P<0.05$, statistically significant differences. OS, osteosarcoma.

OS tissues compared to the adjacent normal bone tissues ($P<0.05$, Fig. 1A). Subsequently, we examined the association between miR-873 expression and the clinicopathological characteristics of the patients with OS. As shown in Table I, a low miR-873 expression was significantly associated with tumor size ($P=0.015$), clinical stage ($P=0.032$) and distant metastasis ($P=0.015$). However, no obvious association between miR-873 expression and other clinicopathological characteristics of the OS patients was observed, i.e., age at diagnosis, sex and anatomical location (each $P>0.05$). RT-qPCR analysis was also carried out to measure the

miR-873 expression levels in a panel of OS cell lines (MG-63, SAOS-2, HOS and U2OS). The results revealed that miR-873 expression was downregulated in all 4 OS cell lines compared to the normal human hFOB1.19 osteoblasts ($P<0.05$, Fig. 1B). These data suggest that miR-873 plays a crucial role in OS progression.

miR-873 overexpression suppresses OS cell growth in vitro. To clarify the role of miR-873 in the development of OS, we selected the HOS and U2OS cell lines, which expressed particularly low levels of miR-873 among the 4 OS cell lines examined (Fig. 1B), for functional experiments. We transfected the HOS and U2OS cells with miR-873 mimics or miR-NC. Following transfection, RT-qPCR analysis demonstrated that miR-873 was markedly overexpressed in the HOS and U2OS cells following transfection with the miR-873 mimics ($P<0.05$, Fig. 2A). We then carried out a CCK-8 assay to examine the proliferation of the HOS and U2OS cells transfected with miR-873 mimics or miR-NC. The results indicated that the proliferation of both cell lines was significantly suppressed when miR-873 was upregulated ($P<0.05$, Fig. 2B). Our subsequent evaluation of the colony formation ability revealed fewer colonies of the HOS and U2OS cells following transfection with miR-873 mimics ($P<0.05$, Fig. 2C). We also used flow cytometric analysis to verify whether the promotion of cell apoptosis suppressed cell proliferation. The results clearly revealed that the apoptotic rate increased in the miR-873 mimic-transfected HOS and U2OS cells compared to the cells transfected with miR-NC ($P<0.05$, Fig. 2D). These results indicate that miR-873 overexpression suppresses OS cell growth *in vitro*.

miR-873 upregulation impairs OS cell migration and invasion in vitro. We carried out Transwell migration and invasion assays to determine whether miR-873 affects the metastatic ability of the OS cells. As shown in Fig. 3A, the ectopic expression of miR-873 suppressed the migration of the HOS and U2OS cells compared with the migration of the cells in the miR-NC groups ($P<0.05$). Furthermore, the invasive ability of the miR-873 mimic-transfected HOS and U2OS cells was markedly lower in comparison with that of the miR-NC-transfected cells ($P<0.05$, Fig. 3B). These results suggest that miR-873 suppresses OS cell metastasis *in vitro*.

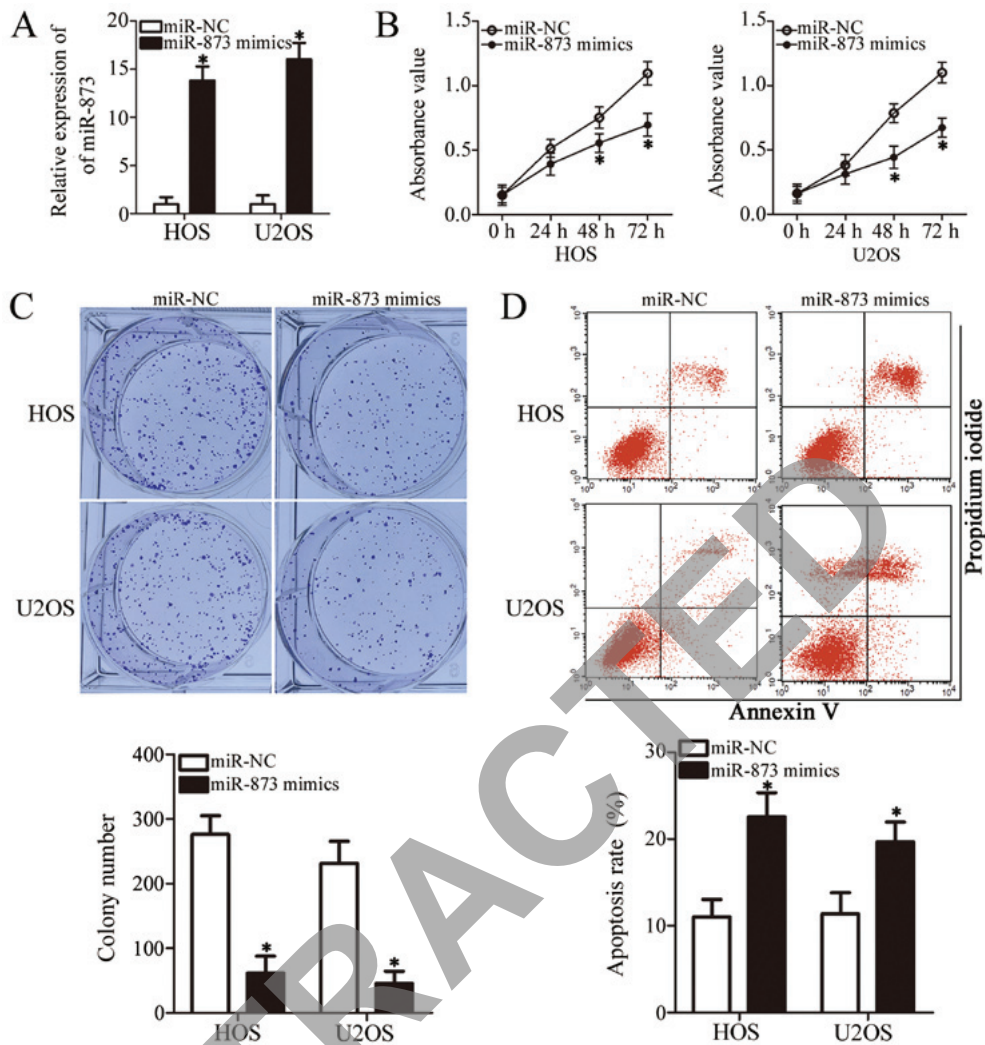


Figure 2. Overexpression of miR-873 suppresses osteosarcoma (OS) cell proliferation and colony formation, and induces apoptosis *in vitro*. HOS and U2OS cells were transfected with miR-873 mimics or miR-NC. (A) We carried out reverse transcription-quantitative polymerase chain reaction (RT-qPCR) analysis 48 h after transfection to measure miR-873 expression. * $P < 0.05$ vs. miR-NC. (B and C) We used CCK-8 and colony formation assays to determine the effects of miR-873 upregulation on OS cell proliferation and colony formation, respectively. * $P < 0.05$ vs. miR-NC. (D) We used flow cytometric analysis to determine the rate of apoptosis. * $P < 0.05$ vs. miR-NC.

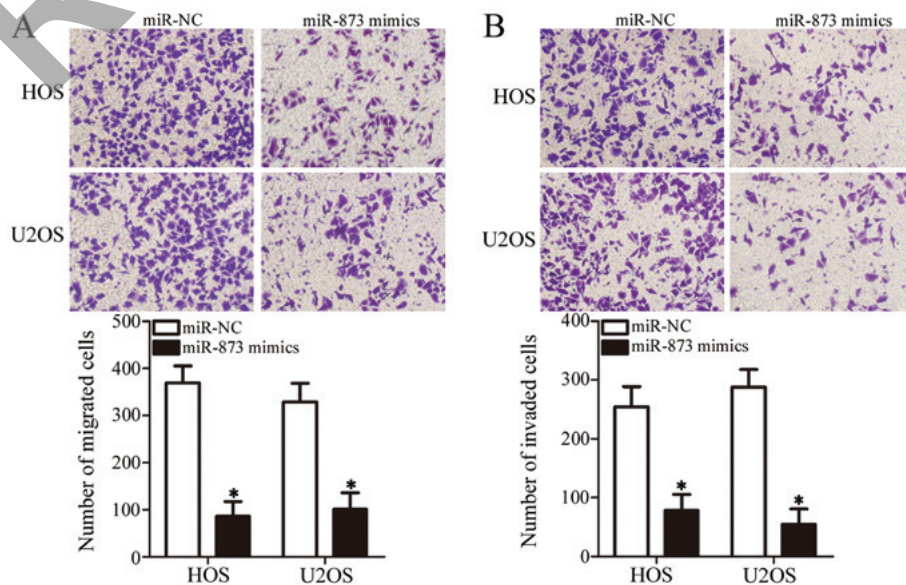


Figure 3. miR-873 upregulation suppresses the migration and invasion of osteosarcoma (OS) cells *in vitro*. We carried out Transwell migration and invasion assays to determine the effects of miR-873 upregulation on HOS and U2OS cell (A) migration and (B) invasion. * $P < 0.05$ vs. miR-NC.

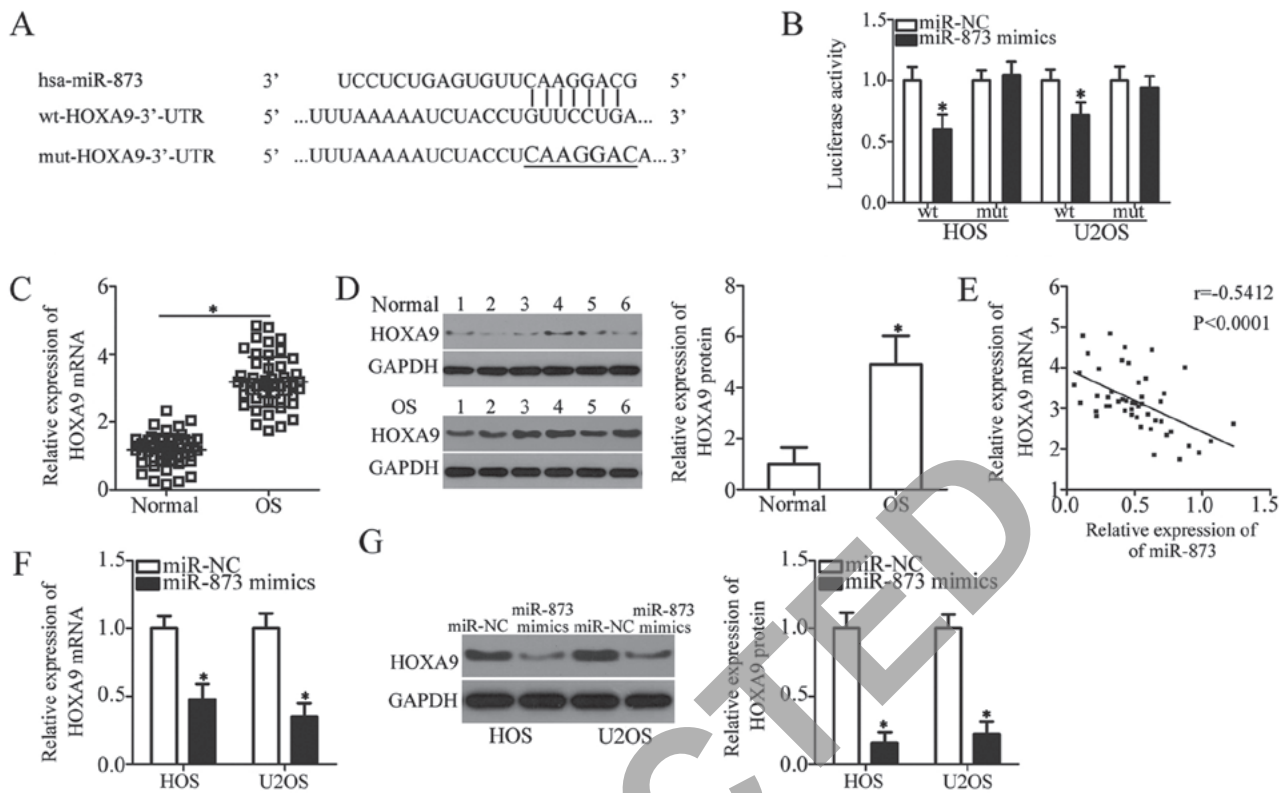


Figure 4. miR-873 negatively regulates *HOXA9* expression in osteosarcoma (OS) cells by directly targeting its 3'-untranslated region (3'-UTR). (A) We used TargetScan 7.1, miRanda and miRDB to predict potential gene targets of miR-873. The wild-type (wt) and mutant binding sites of miR-873 in the 3'-UTR of *HOXA9* are shown. (B) We determined the relative luciferase activity in HOS and U2OS cells following co-transfection with pMIR-wt-*HOXA9*-3'-UTR and pMIR-mut-*HOXA9*-3'-UTR, and miR-873 mimics or miR-NC. * $P < 0.05$ vs. miR-NC. (C and D) We used reverse transcription-quantitative polymerase chain reaction (RT-qPCR) and western blot analyses to determine the expression levels of *HOXA9* mRNA and *HOXA9* protein, respectively, in the OS tissues and adjacent normal bone tissues. * $P < 0.05$ vs. normal adjacent normal bone tissues. (E) We used Spearman's correlation analysis to examine the correlation between miR-873 and *HOXA9* mRNA levels in the OS tissues ($r = -0.5412$, $P < 0.0001$). (F and G) Following the downregulation of miR-873 expression in HOS and U2OS cells, we used RT-qPCR and western blot analyses to determine the expression levels of *HOXA9* mRNA and *HOXA9* protein, respectively. * $P < 0.05$ vs. miR-NC.

HOXA9 is a direct target gene of miR-873 in the OS cells. To illustrate the molecular mechanisms responsible for the miR-873-induced regulation of cell growth and metastasis in OS, we used 3 miRNA target prediction software packages (TargetScan 7.1, miRanda, and miRDB) to predict the putative target(s) of miR-873. We identified an miR-873 binding site in the 3'-UTR of *HOXA9* (Fig. 4A). Among hundreds of candidates, *HOXA9* was selected for further identification owing to its importance in carcinogenesis and cancer progression (30-34). To confirm the prediction mentioned above, we carried out a luciferase reporter assay to verify whether miR-873 was able to recognize and target the 3'-UTR of *HOXA9*. The results revealed that the enhanced expression of miR-873 reduced the luciferase activity of the wild-type *HOXA9* 3'-UTR ($P < 0.05$); however, this inhibition was not observed in the HOS and U2OS cells transfected with mutant *HOXA9* 3'-UTR (Fig. 4B).

We then measured *HOXA9* expression in the OS tissues and assessed its association with the miR-873 levels. The results of RT-qPCR and western blot analyses revealed a substantially upregulated *HOXA9* mRNA ($P < 0.05$, Fig. 4C) and protein ($P < 0.05$, Fig. 4D) expression in the OS tissues compared to the adjacent normal bone tissues. We also examined the correlation between the miR-873 and *HOXA9* mRNA levels using Spearman's correlation analysis, which established

that *HOXA9* mRNA expression inversely correlated with miR-873 expression in the OS tissues ($r = -0.5412$, $P < 0.0001$; Fig. 4E). We found that the levels of *HOXA9* mRNA ($P < 0.05$, Fig. 4F) and *HOXA9* protein ($P < 0.05$, Fig. 4G) were significantly downregulated in the HOS and U2OS cells following the upregulation of miR-873 by transfection with miR-873 mimics. Collectively, these data identify *HOXA9* as a direct target gene of miR-873 in OS cells.

HOXA9 knockdown simulates the tumor suppressor activity of miR-873 in the OS cells. To define the functional role of *HOXA9* in OS cells, we introduced *HOXA9* siRNA into the HOS and U2OS cells to knockdown *HOXA9* expression. Again, NC siRNA was the negative control. The results of western blot analysis demonstrated that *HOXA9* expression was markedly downregulated in the HOS and U2OS cells transfected with *HOXA9* siRNA ($P < 0.05$, Fig. 5A). The results of CCK-8 and colony formation assays indicated that *HOXA9* downregulation significantly inhibited both the proliferation ($P < 0.05$, Fig. 5B) and colony formation ($P < 0.05$, Fig. 5C) of the HOS and U2OS cells. The apoptotic rate of the HOS and U2OS cells also increased following transfection with *HOXA9* siRNA, as detected by flow cytometric analysis ($P < 0.05$, Fig. 5D). Furthermore, the results of Transwell migration and invasion assays revealed that the silencing of *HOXA9*

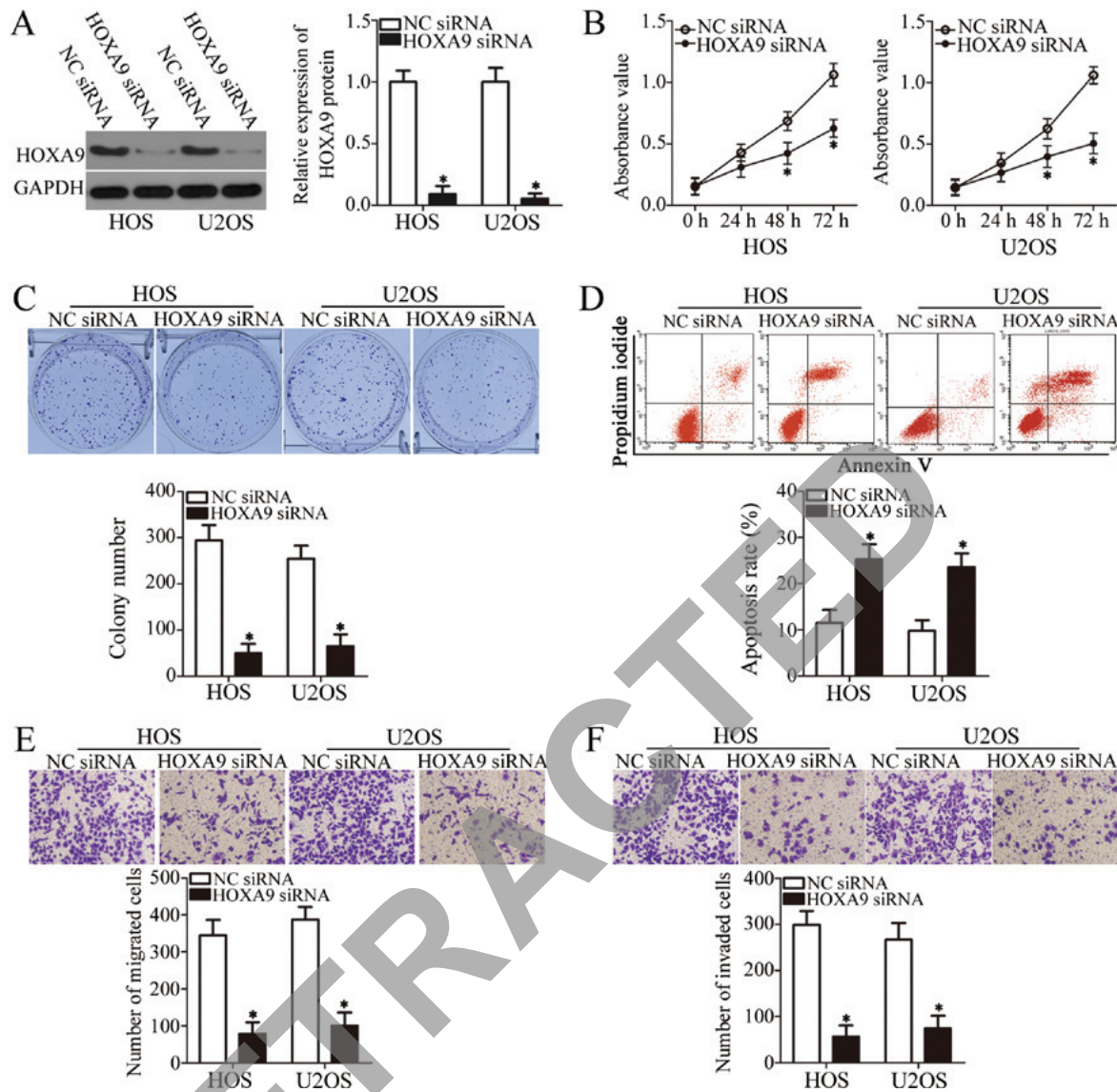


Figure 5. The effects of HOXA9 silencing on osteosarcoma (OS) cells were similar to those induced by miR-873 overexpression. (A) We determined HOXA9 protein expression levels by western blot analysis in HOS and U2OS cells transfected with HOXA9 siRNA or NC siRNA. *P<0.05 vs. miR-NC. (B and C) We assessed the effects of HOXA9 knockdown on HOS and U2OS cell proliferation and colony formation with CCK-8 and colony formation assays, respectively. *P<0.05 vs. NC siRNA. (D) We carried out flow cytometric analysis to determine the apoptotic rate of HOS and U2OS cells following transfection with HOXA9 siRNA or NC siRNA. *P<0.05 vs. NC siRNA. (E and F) We determined the migratory and invasive abilities of HOS and U2OS cells transfected with HOXA9 siRNA or NC siRNA by Transwell migration and invasion assays. *P<0.05 vs. NC siRNA.

suppressed the migratory (P<0.05, Fig. 5E) and invasive (P<0.05, Fig. 5F) capabilities of both cell lines. Therefore, HOXA9 knockdown affected the OS cells in a similar manner to miR-873 upregulation, further suggesting that HOXA9 is a direct downstream target of miR-873.

HOXA9 re-introduction partially antagonizes the suppressive effects of miR-873 overexpression on OS cells. We carried out rescue experiments to further ascertain whether HOXA9 targeting by miR-873 is responsible for the tumor suppressive role of miR-873 in OS cells. We constructed a HOXA9 overexpression plasmid, pcDNA3.1-HOXA9 (pc-HOXA9). We then co-transfected the HOS and U2OS cells with pc-HOXA9 and the miR-873 mimics. pc-HOXA9 co-transfection reversed the suppressive effects on HOXA9 protein expression induced by transfection with miR-873 mimics (P<0.05, Fig. 6A). The results of functional assays

indicated that miR-873 overexpression suppressed cell proliferation (P<0.05, Fig. 6B) and colony formation (P<0.05, Fig. 6C), while simultaneously inducing apoptosis (P<0.05, Fig. 6D) and suppressing cell migration (P<0.05, Fig. 7A) and invasion (P<0.05, Fig. 7B) *in vitro*. However, the restored expression of HOXA9 abolished all the effects described above. These results clearly demonstrate that miR-873 inhibits the aggressive phenotype of OS cells by directly targeting HOXA9, and that the downregulation of HOXA9 by miR-873 is essential for miR-873-induced tumor suppression in OS cells.

miR-873-induced suppression of HOXA9 results in the inactivation of the Wnt/β-catenin signaling pathway in OS cells in vitro. HOXA9 is involved in the modulation of the Wnt/β-catenin signaling pathway (34,35). Therefore, in this study, we attempted to determine whether the effects

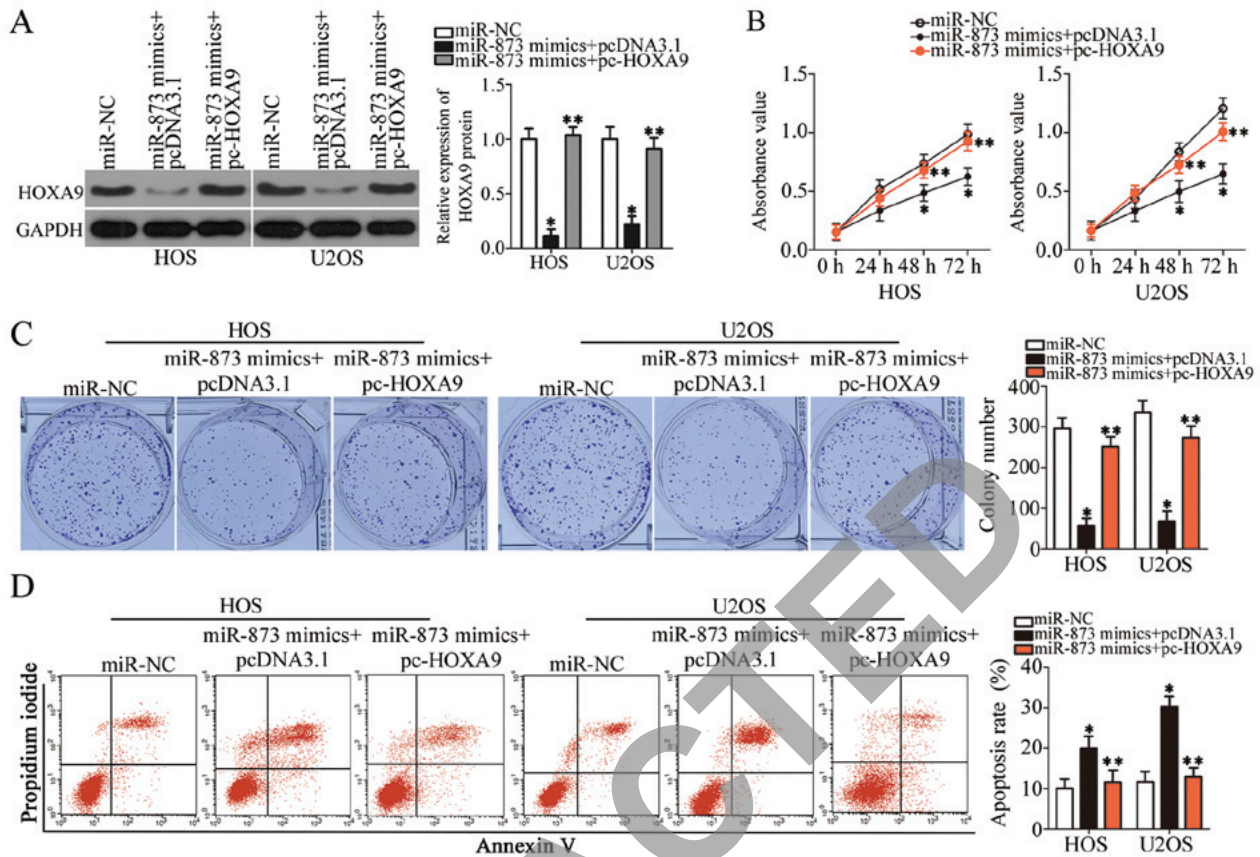


Figure 6. *HOXA9* restoration partially reverses the tumor suppressive effects of miR-873 on the proliferation, colony formation and apoptosis of osteosarcoma (OS) cells. We further transfected miR-873-overexpressing HOS and U2OS cells with the *HOXA9* overexpression plasmid pcDNA3.1-*HOXA9* (pc-*HOXA9*) or the empty plasmid pcDNA3.1. (A) We carried out western blot analysis to detect *HOXA9* protein expression. * $P < 0.05$ vs. miR-NC. ** $P < 0.05$ vs. miR-873 mimics + pcDNA3.1. (B-D) We assessed the proliferation, colony formation and apoptosis status of the above-mentioned cells with a CCK-8 assay, a colony formation assay and flow cytometric analysis, respectively. * $P < 0.05$ vs. miR-NC. ** $P < 0.05$ vs. miR-873 mimics + pcDNA3.1.

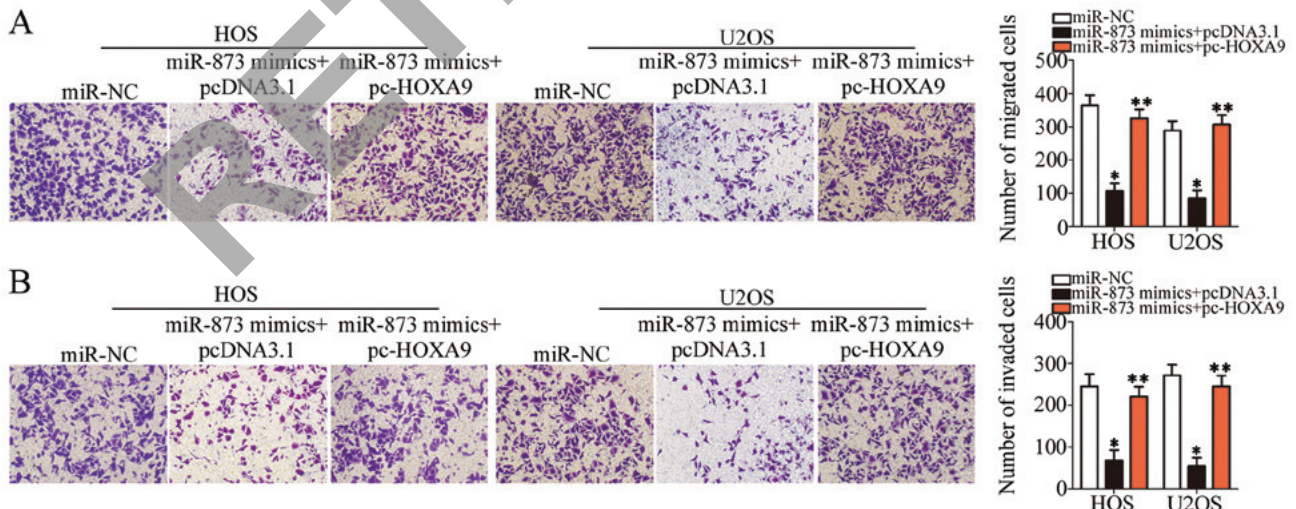


Figure 7. Modulation of *HOXA9* partially reverses the miR-873-mediated suppression of osteosarcoma (OS) cell migration and invasion. (A and B) We used Transwell migration and invasion assays to evaluate the (A) migration and (B) invasion of HOS and U2OS cells co-transfected with miR-873 mimics and pc-*HOXA9* or pcDNA3.1. * $P < 0.05$ vs. miR-NC. ** $P < 0.05$ vs. miR-873 mimics + pcDNA3.1.

of miR-873 on *HOXA9* have an impact on the activation of the Wnt/ β -catenin signaling pathway in OS cells. We transfected the HOS and U2OS cells with miR-873 in combination with pc-*HOXA9* or pcDNA3.1. Following transfection, we used western blot analysis to determine

the expression levels of certain proteins that are involved in the Wnt/ β -catenin pathway, such as p- β -catenin, β -catenin and cyclin D1. The results revealed that the expression levels of both p- β -catenin and cyclin D1 decreased in the HOS and U2OS cells when miR-873 was overexpressed.

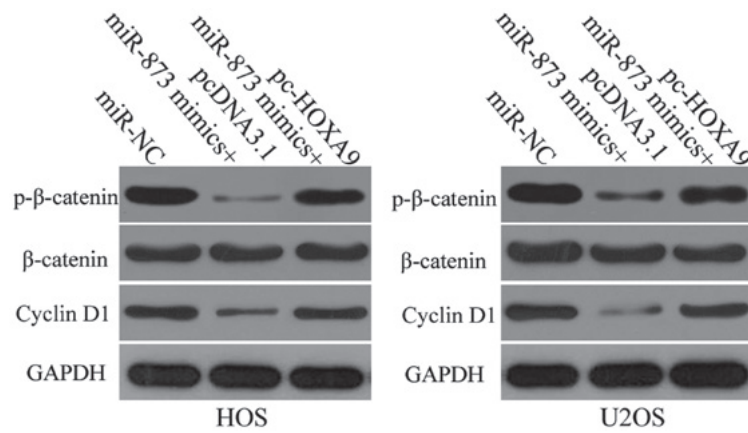


Figure 8. miR-873 inhibits the activation of the Wnt/ β -catenin pathway in osteosarcoma (OS) cells. We co-transfected HOS and U2OS cells with miR-873 mimics and pc-HOXA9 or pcDNA3.1, and used western blot analysis to detect p- β -catenin, β -catenin, and cyclin D1 expression at 72 h following transfection.

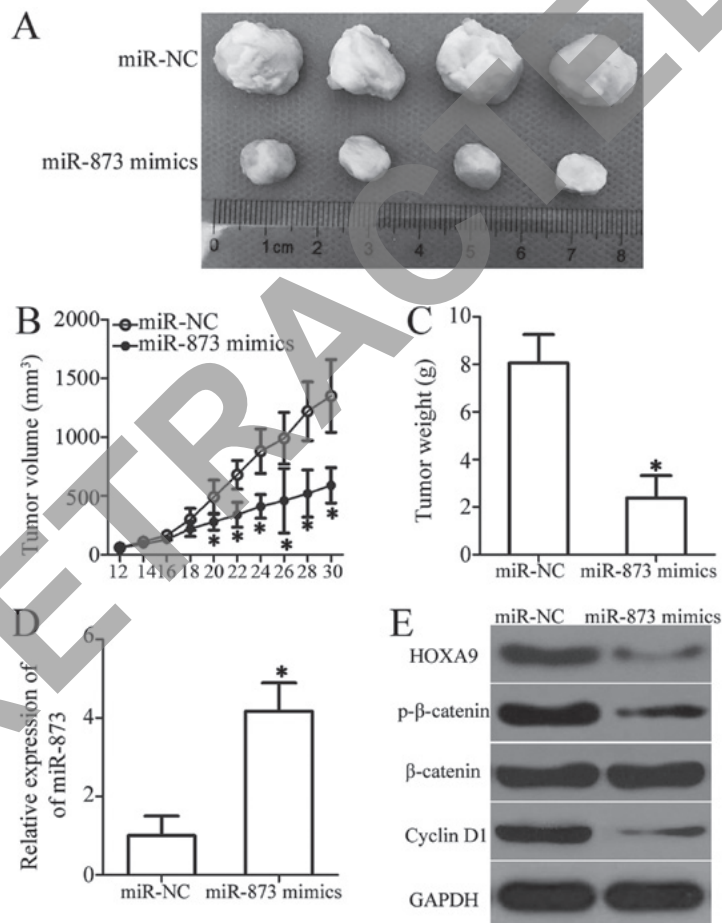


Figure 9. miR-873 hinders osteosarcoma (OS) tumor growth *in vivo*. (A and B) Tumor volumes of xenografts from miR-873 mimics-transfected and miR-NC-transfected cells. * $P < 0.05$ vs. miR-NC. (C) Tumor weights of xenografts measured 30 days after seeding. * $P < 0.05$ vs. miR-NC. (D) We used reverse transcription-quantitative polymerase chain reaction (RT-qPCR) analysis to detect miR-873 expression in the tumor xenografts. * $P < 0.05$ vs. miR-NC. (E) We used western blot analysis to determine protein expression levels of HOXA9, p- β -catenin, β -catenin and cyclin D1.

However, the ectopic overexpression of miR-873 had no effect on total β -catenin protein expression. Furthermore, *HOXA9* overexpression was able to restore p- β -catenin and cyclin D1 expression in the miR-873-transfected HOS and U2OS cells (Fig. 8). These results suggest that miR-873 deactivates the Wnt/ β -catenin pathway in OS cells by directly targeting *HOXA9*.

miR-873 suppresses the tumor growth of OS cells in vivo. We used a tumor xenograft assay to determine the influence of miR-873 on OS cell tumor growth *in vivo*. We subcutaneously injected HOS cells transfected with miR-873 mimics or miR-NC into the upper flanks of nude mice. The volumes ($P < 0.05$, Fig. 9A and B) and weights ($P < 0.05$, Fig. 9C) of the tumor xenografts derived from the miR-873-overexpressing

cells were significantly lower than those derived from the miR-NC-transfected cells. Moreover, there was a sharp increase in the selective expression of miR-873 in the tumor xenografts of the miR-873 mimics group, as determined by RT-qPCR analysis ($P < 0.05$, Fig. 9D). Furthermore, western blot analysis of the tumor xenografts revealed the marked downregulation of HOXA9, p- β -catenin and cyclin D1 expression in the miR-873 mimics group (Fig. 9E). These data suggest that miR-873 suppresses the growth of OS cells *in vivo*, and identify the downregulation of HOXA9 and the subsequent inactivation of the Wnt/ β -catenin pathway as possible underlying mechanisms.

Discussion

Aberrantly expressed miRNA can lead to the development of various diseases, including human malignancies (36). Several miRNAs have been found to be dysregulated in OS, including miR-125b (15), miR-150 (37), miR-214 (38) and miR-1301 (39). Dysregulated miRNA expression may affect a variety of cancer-related biological processes, resulting in the development and progression of OS. Therefore, an in-depth evaluation of the role of specific miRNAs in OS may prove to be a valuable approach with which to identify suitable therapeutic targets. To the best of our knowledge, the present study is the first to investigate the expression pattern, clinical relevance, detailed roles and implied molecular mechanisms of action of miR-873 in OS.

miR-873 is highly expressed in non-small cell lung cancer tissues and cell lines (21,22). By contrast, miR-873 levels are relatively low in colorectal cancer. The downregulation of miR-873 is clearly associated with the tumor stage in patients with colorectal cancer (23), and the expression level of miR-873 is recognized as a biomarker that predicts shorter overall survival rates (23). The expression of miR-873 is also downregulated in gastric cancer (24), esophageal cancer (25), breast cancer (26), ovarian cancer (27) and glioblastoma (28). The heterogeneous expression pattern of miR-873 is of interest to us, along with its clinical value. In the present study, we carried out RT-qPCR analysis to determine the expression levels of miR-873 in OS tissues and cell lines. The results revealed that miR-873 was poorly expressed in the OS tissues and cell lines. The reduced expression of miR-873 was associated with tumor size, clinical stage and distant metastasis. These findings suggest that miR-873 is an effective diagnostic biomarker for the aforementioned types of human cancer.

miR-873 serves as an oncogene in non-small cell lung cancer. For example, miR-873 overexpression increases the proliferation and migration of lung adenocarcinoma cells by directly targeting SRC kinase signaling inhibitor 1 (SRCIN1) (22). Moreover, the downregulation of miR-873 improves the chemosensitivity of non-small cell lung cancer cells to gefitinib through regulation of GLI1 (21). However, miR-873 plays a tumor suppressive role in many other types of cancer. Consistently, restoring miR-873 expression prevents the growth and metastasis of esophageal cancer via a DEC2 blockade (25). Furthermore, miR-873 directly targets ATP-binding cassette subfamily B member 1 (ABCB1), thereby improving the chemosensitivity of ovarian cancer cells

to cisplatin and paclitaxel (27). miR-873 also functions as a tumor suppressor in gastric cancer (24), breast cancer (26), and glioblastoma (28). These conflicting observations suggest that the functional roles of miR-873 in tumorigenesis and tumor development are tissue-specific. However, the role of miR-873 in OS progression remains largely unexplored. In the present study, a series of functional experiments demonstrated that the restoration of miR-873 expression suppressed OS cell proliferation and colony formation, induced cell apoptosis, prevented cell migration and invasion *in vitro*, and hampered tumor growth *in vivo*. Therefore, miR-873 may be a promising potential therapeutic target for patients affected by a number of different cancer types.

The identification of the direct targets of miR-873 is important, not only to clarify its role as a regulator of OS progression, but also for the development of effective therapies. In the present study, we investigated the underlying molecular mechanisms through which miR-873 may affect the aggressive behavior of OS cells. Firstly, bioinformatics prediction identified HOXA9 as a potential target of miR-873. Secondly, a luciferase reporter assay revealed that the 3'-UTR of HOXA9 was recognized and targeted by miR-873 in the OS cells. Thirdly, we found that HOXA9 expression was upregulated in OS tissues, and inversely correlated with miR-873 expression. Fourthly, miR-873 overexpression reduced endogenous HOXA9 expression in the OS cells at the mRNA and protein level. Fifthly, HOXA9 silencing mimicked the effects of miR-873 overexpression on OS cells. Finally, the restored expression of HOXA9 was able to partially abrogate the suppressive effects of miR-873 upregulation on OS cells. Collectively, these data demonstrate that miR-873 directly targets HOXA9 to inhibit the malignant progression of OS cells.

HOXA9, a member of the mammalian HOX family (40), plays a crucial role in the development of healthy limbs, skeletons, mammary glands, urogenital tracts, and kidneys (41). The aberrant activation of HOXA9 has been reported in multiple human cancer types, including gastric cancer (30), colorectal cancer (31), bladder cancer (32), and glioblastoma (33). HOXA9 is also upregulated in OS tissues, and contributes to the formation and progression of OS by regulating a variety of cancer-associated behaviors, including cell proliferation, the regulation of the cell cycle and apoptosis, cell migration *in vitro* and tumor growth *in vivo* (34). The present study demonstrated that miR-873 directly targeted HOXA9 and attenuated the malignant phenotype of OS cells, both *in vitro* and *in vivo*, through the inactivation of the Wnt/ β -catenin signaling pathway. Hence, HOXA9 silencing via miR-873 restoration may prove to be a potential therapeutic approach for the treatment of patients with OS.

In conclusion, the present study demonstrates that miR-873 plays a tumor suppressive role in the progression and development of OS by directly targeting HOXA9. These observations have enhanced our understanding of OS pathogenesis, and we therefore intend to evaluate novel therapeutic targets for the treatment of patients with this disease in the near future.

Acknowledgements

Not applicable.

Funding

No funding was received.

Availability of data and materials

The datasets used and/or analyzed during the present study are available from the corresponding author on reasonable request.

Authors' contributions

YL and YW conceived and designed the study. YW, HY and LZ performed the RT-qPCR, the CCK-8 assay, flow cytometry analysis, and the luciferase reporter assay. Other functional experiments were carried out by RS, HT and LW. All the authors have read and approved the final draft of this manuscript.

Ethics approval and consent to participate

The present study was approved by the Ethics Committee of the First Affiliated Hospital of Zhengzhou University, and was performed in accordance with the Declaration of Helsinki and the guidelines of the Ethics Committee of the First Affiliated Hospital of Zhengzhou University. All patients provided written informed consent. All experimental procedures involving animals were approved by the Ethics Review Committee of the First Affiliated Hospital of Zhengzhou University.

Patient consent for publication

Not applicable.

Competing interests

The authors declare that they have no competing interests.

References

1. Ta HT, Dass CR, Choong PF and Dunstan DE: Osteosarcoma treatment: State of the art. *Cancer Metastasis Rev* 28: 247-263, 2009.
2. Tang J, Shen L, Yang Q and Zhang C: Overexpression of metadherin mediates metastasis of osteosarcoma by regulating epithelial-mesenchymal transition. *Cell Prolif* 47: 427-434, 2014.
3. Gorlick R and Khanna C: Osteosarcoma. *J Bone Miner Res* 25: 683-691, 2010.
4. Berman SD, Calo E, Landman AS, Danielian PS, Miller ES, West JC, Fonhoue BD, Caron A, Bronson R, Boussein ML, *et al*: Metastatic osteosarcoma induced by inactivation of Rb and p53 in the osteoblast lineage. *Proc Natl Acad Sci USA* 105: 11851-11856, 2008.
5. Tang N, Song WX, Luo J, Haydon RC and He TC: Osteosarcoma development and stem cell differentiation. *Clin Orthop Relat Res* 466: 2114-2130, 2008.
6. Farfalli GL, Albergio JJ, Lobos PA, Smith DE, Streitenberger PD, Pallotta Rodríguez MG and Aponte-Tinao LA: Osteosarcoma lung metastases. Survival after chemotherapy and surgery. *Medicina (B Aires)* 75: 87-90, 2015 (In Spanish).
7. Lindsey BA, Markel JE and Kleinerman ES: Osteosarcoma Overview. *Rheumatol Ther* 4: 25-43, 2017.
8. Ottaviani G and Jaffe N: The epidemiology of osteosarcoma. *Cancer Treat Res* 152: 3-13, 2009.
9. Ma O, Cai WW, Zender L, Dayaram T, Shen J, Herron AJ, Lowe SW, Man TK, Lau CC and Donehower LA: MMP13, Birc2 (cIAP1), and Birc3 (cIAP2), amplified on chromosome 9, collaborate with p53 deficiency in mouse osteosarcoma progression. *Cancer Res* 69: 2559-2567, 2009.
10. Bartel DP: MicroRNAs: Genomics, biogenesis, mechanism, and function. *Cell* 116: 281-297, 2004.
11. Gee HE, Ivan C, Calin GA and Ivan M: HypoxamiRs and cancer: from biology to targeted therapy. *Antioxid Redox Signal*. 21: 1220-1238, 2014.
12. Aigner A: MicroRNAs (miRNAs) in cancer invasion and metastasis: Therapeutic approaches based on metastasis-related miRNAs. *J Mol Med (Berl)* 89: 445-457, 2011.
13. Cho WC: MicroRNAs: Potential biomarkers for cancer diagnosis, prognosis and targets for therapy. *Int J Biochem Cell Biol* 42: 1273-1281, 2010.
14. Yang F, Ning Z, Ma L, Liu W, Shao C, Shu Y and Shen H: Exosomal miRNAs and miRNA dysregulation in cancer-associated fibroblasts. *Mol Cancer* 16: 148, 2017.
15. Xiao T, Zhou Y, Li H, Xiong L, Wang J, Wang ZH and Liu LH: miR-125b suppresses the carcinogenesis of osteosarcoma cells via the MAPK-STAT3 pathway. *J Cell Biochem*: 2018 Sep 11, 2018. doi: 10.1002/jcb.27568 (Epub ahead of print).
16. Zhang X, Qian Y, Li F, Bei S, Li M and Feng L: microRNA-9 selectively targets LMX1A to promote gastric cancer cell progression. *Biochem Biophys Res Commun* 505: 405-412, 2018.
17. Song H, Li D, Wu T, Xie D, Hua K, Hu J, Deng X, Ji C, Deng Y and Fang L: MicroRNA-301b promotes cell proliferation and apoptosis resistance in triple-negative breast cancer by targeting CYLD. *BMB Rep* 51: 602-607, 2018.
18. Liao C, Chen W and Wang J: miR-20a regulates glioma cell proliferation, invasion and apoptosis by targeting CELF2. *World Neurosurg* 121: e519-e527, 2019.
19. Kim YH, Goh TS, Lee CS, Oh SO, Kim JI, Jeung SH and Pak K: Prognostic value of microRNAs in osteosarcoma: A meta-analysis. *Oncotarget* 8: 8726-8737, 2017.
20. Kushlinskii NE, Fridman MV and Braga EA: Molecular mechanisms and microRNAs in osteosarcoma pathogenesis. *Biochemistry (Mosc)* 81: 315-328, 2016.
21. Jin S, He J, Li J, Guo R, Shu Y and Liu P: miR-873 inhibition enhances gefitinib resistance in non-small cell lung cancer cells by targeting glioma-associated oncogene homolog 1. *Thorac Cancer* 9: 1262-1270, 2018.
22. Gao Y, Xue Q, Wang D, Du M, Zhang Y and Gao S: miR-873 induces lung adenocarcinoma cell proliferation and migration by targeting SRCIN1. *Am J Transl Res* 7: 2519-2526, 2015.
23. Gong H, Fang L, Li Y, Du J, Zhou B, Wang X, Zhou H, Gao L, Wang K and Zhang J: miR-873 inhibits colorectal cancer cell proliferation by targeting TRAF5 and TAB1. *Oncol Rep* 39: 1090-1098, 2018.
24. Cao D, Yu T and Ou X: miR-873-5P controls gastric cancer progression by targeting hedgehog-GLI signaling. *Pharmazie* 71: 603-606, 2016.
25. Liang Y, Zhang P, Li S, Li H, Song S and Lu B: MicroRNA-873 acts as a tumor suppressor in esophageal cancer by inhibiting differentiated embryonic chondrocyte expressed gene 2. *Biomed Pharmacother* 105: 582-589, 2018.
26. Cui J, Yang Y, Li H, Leng Y, Qian K, Huang Q, Zhang C, Lu Z, Chen J, Sun T, *et al*: miR-873 regulates ER α transcriptional activity and tamoxifen resistance via targeting CDK3 in breast cancer cells. *Oncogene* 34: 4018, 2015.
27. Wu DD, Li XS, Meng XN, Yan J and Zong ZH: MicroRNA-873 mediates multidrug resistance in ovarian cancer cells by targeting ABCB1. *Tumour Biol* 37: 10499-10506, 2016.
28. Wang RJ, Li JW, Bao BH, Wu HC, Du ZH, Su JL, Zhang MH and Liang HQ: MicroRNA-873 (miRNA-873) inhibits glioblastoma tumorigenesis and metastasis by suppressing the expression of IGF2BP1. *J Biol Chem* 290: 8938-8948, 2015.
29. Livak KJ and Schmittgen TD: Analysis of relative gene expression data using real-time quantitative PCR and the 2⁻(Delta Delta C(T)) Method. *Methods* 25: 402-408, 2001.
30. Ma YY, Zhang Y, Mou XZ, Liu ZC, Ru GQ and Li E: High level of homeobox A9 and PBX homeobox 3 expression in gastric cancer correlates with poor prognosis. *Oncol Lett* 14: 5883-5889, 2017.
31. Wang X, Bu J, Liu X, Wang W, Mai W, Lv B, Zou J, Mo X, Li X, Wang J, *et al*: miR-133b suppresses metastasis by targeting HOXA9 in human colorectal cancer. *Oncotarget* 8: 63935-63948, 2017.
32. Kim YJ, Yoon HY, Kim JS, Kang HW, Min BD, Kim SK, Ha YS, Kim IY, Ryu KH, Lee SC, *et al*: HOXA9, ISL1 and ALDH1A3 methylation patterns as prognostic markers for nonmuscle invasive bladder cancer: Array-based DNA methylation and expression profiling. *Int J Cancer* 133: 1135-1142, 2013.

33. Costa BM, Smith JS, Chen Y, Chen J, Phillips HS, Aldape KD, Zardo G, Nigro J, James CD, Fridlyand J, *et al*: Reversing HOXA9 oncogene activation by PI3K inhibition: Epigenetic mechanism and prognostic significance in human glioblastoma. *Cancer Res* 70: 453-462, 2010.
34. Zhang ZF, Wang YJ, Fan SH, Du SX, Li XD, Wu DM, Lu J and Zheng YL: MicroRNA-182 downregulates Wnt/ β -catenin signaling, inhibits proliferation, and promotes apoptosis in human osteosarcoma cells by targeting HOXA9. *Oncotarget* 8: 101345-101361, 2017.
35. Fu Z, Chen C, Zhou Q, Wang Y, Zhao Y, Zhao X, Li W, Zheng S, Ye H, Wang L, *et al*: LncRNA HOTTIP modulates cancer stem cell properties in human pancreatic cancer by regulating HOXA9. *Cancer Lett* 410: 68-81, 2017.
36. Hosseinahli N, Aghapour M, Duijf PHG and Baradaran B: Treating cancer with microRNA replacement therapy: A literature review. *J Cell Physiol* 233: 5574-5588, 2018.
37. Wang L, Aireti A, Aihaiti A and Li K: Expression of microRNA-150 and its Target Gene IGF2BP1 in Human Osteosarcoma and their Clinical Implications. *Pathol Oncol Res*: Sep 15, 2018 (Epub ahead of print). doi: 10.1007/s12253-018-0454-0.
38. Rehei AL, Zhang L, Fu YX, Mu WB, Yang DS, Liu Y, Zhou SJ and Younusi A: MicroRNA-214 functions as an oncogene in human osteosarcoma by targeting TRAF3. *Eur Rev Med Pharmacol Sci* 22: 5156-5164, 2018.
39. Wang L, Hu K and Chao Y: MicroRNA-1301 inhibits migration and invasion of osteosarcoma cells by targeting BCL9. *Gene* 679: 100-107, 2018.
40. Lawrence HJ, Christensen J, Fong S, Hu YL, Weissman I, Sauvageau G, Humphries RK and Largman C: Loss of expression of the Hoxa-9 homeobox gene impairs the proliferation and repopulating ability of hematopoietic stem cells. *Blood* 106: 3988-3994, 2005.
41. Kmita M, Tarchini B, Zàkány J, Logan M, Tabin CJ and Duboule D: Early developmental arrest of mammalian limbs lacking HoxA/HoxD gene function. *Nature* 435: 1113-1116, 2005.

RETRACTED